

Feature Analyses and Modeling of Lithium-Ion Battery Manufacturing Based on Random Forest Classification

Kailong Liu , Member, IEEE, Xaosong Hu , Senior Member, IEEE, Huiyu Zhou , Lei Tong, W. Dhammika Widanage , Member, IEEE, and James Marco

Abstract—Lithium-ion battery manufacturing is a highly complicated process with strongly coupled feature inter-dependencies; a feasible solution that can analyze feature variables within manufacturing chain and achieve reliable classification is, thus, urgently needed. This article proposes a random forest (RF)-based classification framework, through using the out of bag predictions, Gini changes, as well as predictive measure of association (PMOA), for effectively quantifying the importance and correlations of battery manufacturing features and their effects on the classification of electrode properties. Battery manufacturing data containing three intermediate product features from the mixing stage and one product parameter from the coating stage are analyzed by the designed RF framework to investigate their effects on both the battery electrode active material mass load and porosity. Illustrative results demonstrate that the proposed RF framework not only achieves the reliable classification of electrode properties, but also leads to the effective quantification of both manufacturing feature importance (FI) and correlations. This is the first time to design a systematic RF framework for simultaneously quantifying battery production FI and correlations by three various quantitative indicators, including the unbiased FI, gain improvement FI, and PMOA, paving a promising solution to reduce model dimension and conduct efficient sensitivity analysis of battery manufacturing.

Index Terms—Battery manufacturing and management, battery product classification, data-driven model, feature analysis, lithium-ion battery.

Manuscript received May 26, 2020; revised August 23, 2020 and November 20, 2020; accepted December 30, 2020. Date of publication January 5, 2021; date of current version December 15, 2021. Recommended by Technical Editor K. Zhu and Senior Editor R. Gao. This work was supported in part by the Faraday Institution through Nextrode project under Grant FIRG015, and in part by the High Value Manufacturing Catapult project under Grant 160080 CORE. (Corresponding authors: Kailong Liu; Xaosong Hu.)

Kailong Liu, W. Dhammika Widanage, and James Marco are with the Warwick Manufacturing Group, University of Warwick, CV4 7AL Coventry, U.K., and also with the Faraday Institution, OX11 0RA Didcot, U.K. (e-mail: Kailong.Liu@warwick.ac.uk, kliu02@qub.ac.uk; Dhammika.Widanage@warwick.ac.uk; James.Marco@warwick.ac.uk).

Xaosong Hu is with the Department of Automotive Engineering, Chongqing University, Chongqing 400044, China (e-mail: xiaosonghu@ieee.org).

Huiyu Zhou and Lei Tong are with the School of Informatics, University of Leicester, LE1 7RH Leicester, U.K. (e-mail: hz143@leicester.ac.uk; lt228@leicester.ac.uk).

Color versions of one or more figures in this article are available at <https://doi.org/10.1109/TMECH.2020.3049046>.

Digital Object Identifier 10.1109/TMECH.2020.3049046

I. INTRODUCTION

A S A CONSEQUENCE of the manufacturing complexity that involves numerous individual process stages, a large number of variables and parameters are generated and coupled during battery manufacturing [1]. These process parameters will highly affect the properties of manufacturing intermediate products, which, in turn, further determine the final battery performance. Unfortunately, due to the complexity, the multiple inter-relations among key processes and control variables are still difficult to be understood. Currently, the analysis of manufacturing variables to improve battery performance is still mainly dependent on the trial and error methods [2]. Therefore, it is vital to develop powerful data analysis solutions for better understanding and evaluating the variable importance, the process interactions within battery manufacturing chain.

With the rapid development of cloud computing and machine learning technologies, artificial intelligence and data-driven-based strategies are becoming powerful tools in many industrial fields. For instance, a genetic-algorithm- and neural-network-based data-driven method was proposed in [3] for smart semiconductor manufacturing. In [4], through considering the machine interactions and operational context, a hybrid data-driven and physics-based framework was derived for modeling manufacturing equipment to improve anomaly detection and diagnosis. For battery applications, numerous data-driven models have been derived to estimate operational states [5]–[8], predict service life [9]–[12], diagnose faults [13], and achieve effective charging [14]–[16] and energy managements [17], [18]. However, all these research studies mainly focus on the *in situ* operation of battery performance without considering the microscopic properties of its production. As battery manufacturing also generates a large amount of data, it should also be a promising way by designing reliable data-driven solutions to analyze and improve processes within it.

In comparison with battery management research, fewer works have been done so far by applying machine learning techniques in the battery manufacturing domain. Among lots of corresponding themes (process monitoring [19], adjustments [20], and analyses [21]) of battery manufacturing, deriving suitable data-driven models to predict and analyze the intermediate products belongs to a significant research challenge. For instances, through analyzing the initial failure mode and effect,

Schnell and Reinhart [22] proposed a data-driven method for the internal decisions of battery manufacturing quality control without considering the link of each quality parameter. Then, in [23], a data-mining concept named the cross-industry standard process (CRISP) together with linear model, neural network, and regression approach are utilized to identify the process dependence and predict the product qualities of battery manufacturing. According to the CRISP concept, Turetskyy *et al.* [24] proposed a decision-tree (DT)-based framework to conduct manufacturing feature selection and regression models for predicting battery maximal capacity. In [25], a multivariate regression approach based on the CRISP concept was also proposed to predict the final battery manufacturing properties and suggest the suitable quality gates. Based upon the defined capability indices, a hierarchical model was proposed in [26] to determine performance indicators of production chain such as battery weight and capacity. Through using a statistical investigation of battery product fluctuations, Hoffmann *et al.* [27] investigated their effects on the manufactured cell capacities. In [28], three common data-driven models, including support vector machine (SVM), DT, and neural network, are utilized to classify the electrode properties. Then, parameter dependencies are analyzed through the 2-D graphs from model and experiment data. For the aforementioned applications, reasonable data-driven analyses of battery manufacturing have been obtained, and several limitations still exist: 1) research works mainly focus on simply using the existing common methodologies to predict battery product properties, lacking of in-depth investigations on the characteristics of adopted machine learning techniques to further enhance their performance and generalization in the battery manufacturing domain; and 2) many works mainly emphasize the accuracy of the developed model, ignoring systematically analyzing its interpretability for battery manufacturing data. For the battery production chain that presents various feature variables, apart from obtaining the predicted output of the utilized model, manufacturers are also very interested in the underlying correlations among different variables and the features that are more crucial for determining the predicted results. Such information can effectively help battery manufacturers optimize their battery products.

Based upon the above discussions, it becomes significantly meaningful to design the interpretable model for effectively predicting battery manufacturing outputs, with reliable intermediate feature analyses being taken into account. To achieve this, a novel data-driven framework based on the improved random forest (RF) classification technique is designed in this study to simultaneously classify battery electrode properties and determine the levels of both feature importance (FI) and correlations. Specifically, some key contributions are made as follows:

- 1) According to a well-labeled battery electrode manufacturing dataset with five classes, an effective RF model structure with the bagging and out of bag (OOB) prediction solutions is designed, bringing the benefits to achieve unbiased classification of battery electrode properties and highly restrain the overfitting phenomenon.
- 2) Through randomly permuting feature observations within OOB and calculating the Gini changes, two different types of FI, including both unbiased FI and gain improvement

FI, can be derived to directly quantify the importance levels of selected mixing and coating features.

- 3) A powerful noise immunity solution named predictive measure of association (PMOA) is designed from the surrogate decision split, which is able to effectively quantify the strength of correlations between all pairs of manufacturing feature variables.
- 4) The developed RF-based approach is analyzed in depth to evaluate the effects of four key variables from the mixing and coating stages on the classifications of two battery product properties—electrode mass load and porosity.

Obviously, through using the proposed RF-based framework, the importance and correlations of all manufacturing feature variables can be well quantified and analyzed. This is the first known application of designing a systematic RF-based framework to not only classify the electrode properties but also quantify the importance and correlations of involved mixing and coating features with three different evaluation criteria. Due to the data-driven nature, this framework can be conveniently extended to other processes of battery manufacturing chain after collecting the available data, paving a promising way for the reliable sensitivity analysis of intermediate features and the improvement of model dimension as well as battery manufacturing process.

The rest of this article is organized as follows. Section II specifies the battery manufacturing chain and several key process steps. Then, the fundamentals behind the RF classification technology, FI/correlation determination, classification model structure and framework, and performance metrics are described in Section III. Section IV details our classification results with the in-depth discussions of feature correlations and importance. Finally, Section V concludes this article.

II. BATTERY MANUFACTURING FUNDAMENTALS

Li-ion battery manufacturing is a long and highly complicated process chain, which mainly consists of electrodes manufacturing, cell assembly, formation, and ageing. Fig. 1 systematically illustrates several key intermediate processes within the battery production chain especially for electrode manufacturing. In general, after preparing active materials, the slurry could be made within a soft blender through a mixing stage. Then, the slurry is coated on the surface of copper or aluminum foils by a comma-gap (CG) coater with several built-in ovens to dry the coating products. Afterward, the anode and cathode electrodes are obtained through calendering and cutting the dried coating products. Then, all components such as electrodes and electrolyte are assembled to produce the basic battery cell. Due to the highly complicated operations within the battery production chain, engineers can control the electrode mass load and porosity more conveniently and easily with the discrete data and class form in real battery manufacturing [29]. An effective classification approach could, thus, benefit battery manufacturer in such a case.

In this context, to design a reliable RF-based classification framework for analyzing the FI and correlations of battery electrode manufacturing, some key intermediate product features (IPFs) and process parameters (PPs) from mixing and coating

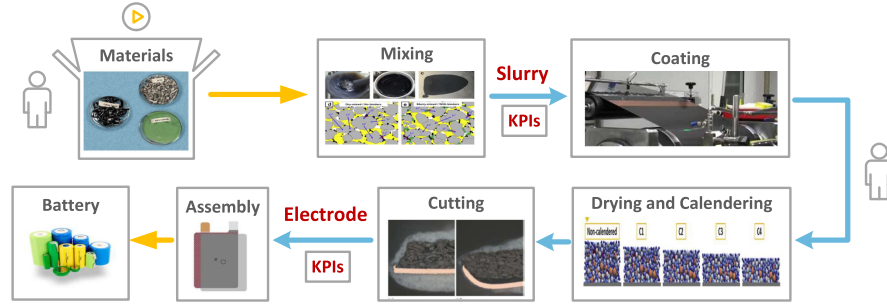


Fig. 1. Key processes within battery production chain especially for electrode manufacturing.

TABLE I
CLASS LABEL SETTING RULES OF BATTERY ELECTRODE MASS LOAD AND POROSITY

Class labels	Mass load [mg/cm ²]	Porosity [%]
very low	≤ 15	≤ 47.5
low	$15 < ML \leq 25$	$47.5 < Po \leq 50$
medium	$25 < ML \leq 35$	$50 < Po \leq 52.5$
high	$35 < ML \leq 45$	$52.5 < Po \leq 55$
very high	> 45	> 55

stages are studied in this article. Besides, their effects on the classification performance of battery electrode characteristics are also investigated. Without loss of generality, the whole raw dataset [28] from the Franco Laboratoire de Reactivite et Chimie des Solides is explored in this study, which leads to that the total number of feature variables here is four. Specifically, these interested battery manufacturing features, including three slurry IPFs (active material mass content (AMMC), solid-to-liquid ratio (StoLR), and viscosity) as well as one coating PP (CG). The StoLR reflects the mass ratio among slurry solids and slurry mass. Viscosity affects the shear rate of coating step. CG represents the gap between comma and coating rolls. For the battery electrode characteristics, two key variables, including the electrode mass load with unit mg/cm² and porosity after drying with unit %, are utilized to reflect the electrode product properties. Detailed information regarding the experiments and data explanations can be found in [28], which is not repeated here due to space limitations. For this raw dataset with 656 samples, eight same samples of slurry IPFs and coating CG are used to generate one related electrode mass load and porosity. Therefore, 82 observations are generated by averaging the related eight samples. To fully investigate the effectiveness of RF classification, both electrode mass load and porosity are classified into multiclass with five labels (very low, low, medium, high, and very high), respectively. The detailed class label setting rules are illustrated in Table I.

Fig. 2 details the number of levels of each features. Obviously, viscosity belongs to a continuous variable with 76 number levels, which is significantly more than other three features (here, the number levels of AMMC, StoLR, and CG is 4, 23, and 6, respectively). Based upon these feature data with large different number levels and preset class labels, the RF-based classification framework is then designed to analyze the importance and correlations of these features in this article.

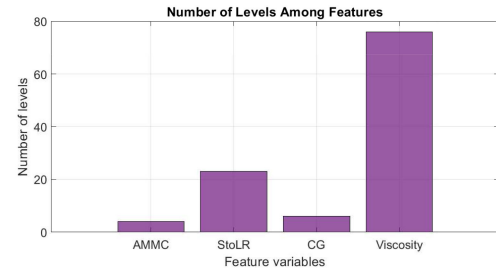


Fig. 2. Number of levels among all interested features.

III. METHODOLOGY

This section first describes the fundamental of RF. Then, the process to conduct feature analyses is elaborated, followed by the description of the RF-based framework to classify battery electrode mass load and porosity. Additionally, the performance metrics to evaluate classification results are also given.

A. Random Forest

Derived from ensemble learning theory, RF combines multiple individual DTs [30]. Due to the simplification and nonparametric behaviors, classification and regression tree (CART) is generally utilized as a DT within RF [31]. Each DT relies on a random bootstrap dataset. The structure of the RF classification model is shown in Fig. 3 [32]. For the classification issue, suppose that training data TD = {(X₁, Y₁), (X₂, Y₂), ..., (X_N, Y_N)} contain N observations, where X_i stands for the input vector with M features as $X_i = (x_{i1}, x_{i2}, \dots, x_{iM})$ and Y_i is the output scalar; the process of establishing an RF classification model is detailed in Workflow 1.

The main purpose of the RF training stage is to construct numerous decorrelated DTs. To decrease the variance associated with classification, an overlap sampling solution named “bagging” is adopted in the RF [32]. Specifically, it extracts observations with replacement to generate the independent bootstrap sample from the training dataset. Then, each DT can be trained from different bootstrap samples, leading to an increased tree diversity. Besides, to further restrain the correlations among various DTs, the best split of each node is obtained through randomly selecting m subset features instead of all M features. As a result, DTs within RF can be grown without pruning, leading to a relatively small computational burden. Moreover,

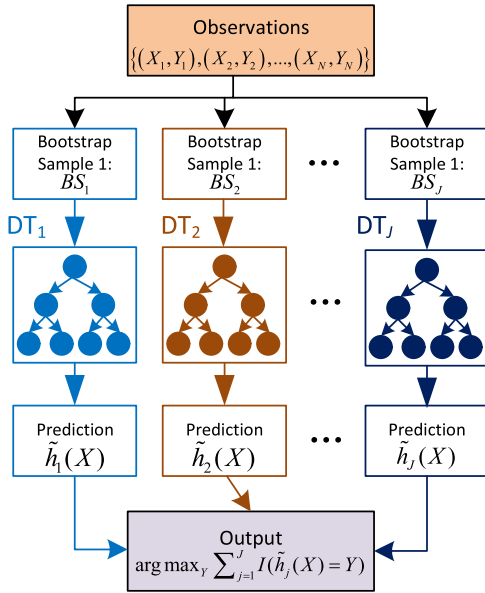


Fig. 3. Structure of RF classification model.

through using different bootstrap samples and node features, the noise immunity of RF can be improved with the help of averaging various decorrelated DTs.

Additionally, for each DT within an RF, due to the bagging solution, some training data would be repeatedly utilized as the bootstrap sample, resulting in some other observations not being selected to fit this DT. These observations are named as OOB samples. In general, nearly one-third TD constitutes OOB samples and would not be utilized in the RF training process. Therefore, at each time when a DT has been trained, the OOB samples can be used to evaluate the classification performance of this DT. In this way, RF is able to achieve unbiased estimations without using external data subset. For the classification of battery product properties, OOB predictions with the related generalization error E_{OOB} of RF can be obtained by Workflow 2.

It should be noticed that the final E_{OOB} is calculated through the error rate of OOB predictions rather than averaging each DT's OOB error. In light of this, a classwise error is obtained for each class, while a confusion matrix (CM) for the classification of battery manufacturing could also be generated.

B. Feature Importance and Correlation

To effectively quantify the importance of both mixing features and coating parameter of battery production, the unbiased FI that is obtained by OOB prediction is first utilized. The detailed process to obtain the unbiased FI is shown in Workflow 3.

In this workflow, $LFM_i(x_k)$ is calculated by averaging over observations with size J_i from the same class, while OFM_{xk} is obtained through averaging over all observations with size N . Therefore, the unbiased importance of feature x_i could reflect how much the classification error varies when the values of x_i are randomly permuted in the OOB prediction tests.

Apart from the unbiased FI, another effective solution to evaluate the importance of features is through summing the gain

Workflow 1: Detailed Process to Establish RF-Based Classification Model.

- 1: **procedure** RF TRAINING
 - 2: For $j = 1$ to J : (J is the number of DTs)
 - 3: Formulate a bootstrap sample BS_j with N observations from TD;
 - 4: Fit a tree DT_j based on its BS_j :
 - a. Start splitting a node with all observations of BS_j .
 - b. Recursively repeat the following processes on each unsplit node:
 - i. Randomly choose m features ($m < M$) from M candidates: $m \leftarrow M$
 - ii. Discover the split solution with the best impurity among all possible splits of m features from Process i.
 - iii. Split this node into two subnodes based on the obtained split solution from Process ii.
 - 5: Obtain the well-trained RF through ensembling all base DT learners $h_j(.)$.
 - 6: **end procedure**
-
- 7: **procedure** RF CLASSIFICATION
 - 8: For a new observation X_{new} , the output $RF(X_{new})$ of RF is predicted by:

$$RF(X_{new}) = \arg \max_Y \sum_{j=1}^J I(\tilde{h}_j(X_{new}) = Y)$$
 where $\tilde{h}_j(X_{new})$ is the j th DT's prediction result with X_{new} as inputs. $I(.)$ is a zero-one judgment with $I(\tilde{h}_j(X_{new}) = Y) = 1$. $\arg \max_Y$ outputs the class with the maximum counting number from all DTs.
 - 9: **end procedure**
-

Workflow 2: OOB Predictions and the Generalization Error.

- 1: **procedure** OOB PREDICTIONS
 - 2: For $i = 1$ to N :
 - i. Suppose $A_i = \{j : (X_i, Y_i) \notin BS_j\}$, and J_i is the cardinality of A_i .
 - ii. Obtain the OOB prediction at X_i by:

$$\tilde{f}_{OOB}(X_i) = \arg \max_Y \sum_{j \in A_i} I(h_j(X_i) = Y)$$
 where $\tilde{h}_j(X_i)$ is the prediction result by using X_i as inputs to the j th DT.
 - 3: Calculate the generalization error E_{OOB} by:

$$E_{OOB} = \frac{1}{N} \sum_{i=1}^N I(Y_i \neq \tilde{f}_{OOB}(X_i))$$
 - 4: **end procedure**
-

improvements of Gini impurity changes caused by the splits on each feature. For the classification, Gini impurity is utilized to measure how well a potential split is in a specific node of DT [33]. The detailed process to obtain the gain improvement FI is illustrated in Workflow 4. Obviously, $I_G(x_k)$ could reflect the gain improvement from the splits of feature x_k . Larger value of $I_G(x_k)$ indicates that this x_k brings higher impurity improvement for the target classification.

On the other hand, evaluating the correlations among various electrode features is also crucial for better understanding battery manufacturing. To achieve this, an effective solution named the PMOA is designed in this study. In theory, the value of PMOA

Workflow 3: Unbiased FI Based on OOB Predictions.

- 1: **procedure** TO ESTIMATE THE UNBIASED IMPORTANCE OF FEATURES $x_k k = 1$ to M
- 2: (Obtain $\tilde{Y}_{i,j}$) For $i = 1$ to N :
 - i. Suppose BS_j is the j th bootstrap sample,
 $A_i = \{j : (X_i, Y_i) \notin BS_j\}$, and J_i is the cardinality of A_i .
 - ii. Obtain $\tilde{Y}_{i,j} = \tilde{h}_j(X_i)$ for all $j \in A_i$.
- 3: (Obtain $\tilde{Y}'_{i,j}$) For $j = 1$ to J :
 - i. Suppose $B_j = \{i : (X_i, Y_i) \notin BS_j\}$
 - ii. Randomly permute x_k from data samples $\{X_i : i \in B_j\}$ to generate $C_j = \{X'_i : i \in B_j\}$.
 - iii. Obtain $\tilde{Y}'_{i,j} = \tilde{h}_j(X'_i)$ for all $i \in B_j$.
- 4: For $i = 1$ to N :
 - Calculate the local FI $LFM_i(x_k)$ of x_k as:

$$LFM_i(x_k) = \frac{1}{J_i} \sum_{j \in A_i} I(Y_i \neq \tilde{Y}'_{i,j}) - \frac{1}{J_i} \sum_{j \in A_i} I(Y_i \neq \tilde{Y}_{i,j})$$
- 5: Obtain the overall unbiased importance (OFM_{xk}) of feature x_k as:

$$OFM_{xk} = \frac{1}{N} \sum_{i=1}^N LFM_i(x_k)$$
- 6: **end procedure**

could reflect the similarities between different decision rules to split observations. The basic idea of obtaining PMOA is to compare all potential splits with the optimal one that is founded by training DT. Then, the best surrogate decision split would generate the maximum PMOA value, which could reflect the correlations between pairs of these two features. Supposing that x_e and x_g are two interested feature variables ($e \neq g$), the detailed equation to calculate PMOA between the optimal split $x_e < u$ and surrogate split $x_g < v$ is expressed as follows:

$$PMOA_{e,g} = \frac{\min(Pl, Pr) - 1 + Pl_{elg} + Pr_{erg}}{\min(Pl, Pr)} \quad (1)$$

where the subscripts l and r represent the left and right children of node, respectively; Pl stands for the observation proportion of $x_e < u$; Pr is the observation proportion of $x_e \geq u$; and Pl_{elg} means the observation proportion of $x_e < u$ and $x_g < v$, while Pr_{erg} represents the observation proportion of $x_e \geq u$ and $x_g \geq v$. For the PMOA, the observations with several missing values of x_e and x_g would not affect the proportion results. $x_g < v$ could be selected as a worthwhile surrogate split for $x_e < u$ when $PMOA_{e,g} > 0$. Besides, the range of PMOA should be within $(-\infty, 1]$, larger PMOA indicates more highly correlated pairs of feature variables.

C. Classification Model Structure and Framework

For the battery manufacturing process, mixing and coating are two key processes to affect electrode properties, further determining the performance of final manufactured battery [29]. To effectively quantify the FI and correlations among all interested variables, an RF classification model with the structure in Fig. 4 is utilized. Specifically, the IPFs of mixing including AMMC, StoLR, and viscosity of slurry, as well as one PP of

Workflow 4: Gain Improvement FI based on Gini changes.

- 1: **procedure** TO ESTIMATE THE GAIN IMPROVEMENT FI OF FEATURES $x_k k = 1$ to M
- 2: (Obtain $\Delta Gini(\tau, x_k)$) For $j = 1$ to J :
 - i. For a node τ of DT_j , calculate its Gini impurity $Gini(\tau)$ by:

$$Gini(\tau) = 1 - \sum_{d=1}^D p_k^2$$
 where D is the number of classes, $p_k = n_k/n$ is the fraction of n_k samples out of total n samples.
 - ii. Calculate all Gini impurities $Gini(\tau, x_i)$ under the case of selected feature x_i by:

$$Gini(\tau, X) = \frac{|\tau_l|}{|\tau|} Gini(\tau_l) + \frac{|\tau_r|}{|\tau|} Gini(\tau_r)$$
 where τ_l and τ_r are the left child and right child of the current node τ , respectively; $|\tau|$, $|\tau_l|$ and $|\tau_r|$ represent the number of records in τ , τ_l , and τ_r , respectively.
 - iii. Calculate the Gini decrease $\Delta Gini(\tau, X)$ of all selected X by:

$$\Delta Gini(\tau, X) = Gini(\tau) - Gini(\tau, X)$$
- iv. Compare $\Delta Gini(\tau, X)$ to obtain the optimal split feature x_k at this specific node τ . Record its Gini decrease $\Delta Gini(\tau, X_k)$.
- 3: (Obtain $I_G(x_k)$) For $j = 1$ to J :
 - i. Accumulate the recorded $\Delta Gini(\tau, x_k)$ for all used nodes (ANs) in all trees (ATs) by:

$$S\Delta Gini(x_k) = \sum_{ATs} \sum_{ANs} \Delta Gini(\tau, x_k)$$
 where $S\Delta Gini(x_k)$ is the summed gain improvement based on x_k 's Gini changes.
 - ii. Calculate the overall gain improvement $I_G(x_k)$ of feature x_k as:

$$I_G(x_k) = \frac{1}{N_{xk}} S\Delta Gini(x_k)$$
 where N_{xk} is the cardinality of $S\Delta Gini(x_k)$.
- 4: **end procedure**

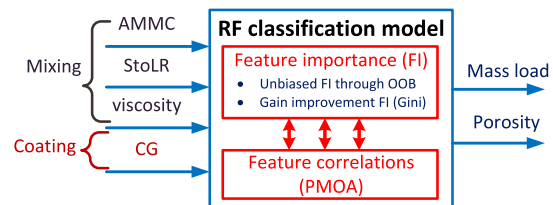


Fig. 4. RF-based classification model structure.

coating named CG are utilized as the inputs, while the output of RF is the labeled classes of electrode mass load or porosity. Fig. 5 illustrates the total framework to design an RF model for classifying and analyzing the FI as well as feature correlations under the specific input–output pairs of battery manufacturing. This framework consists of four main parts and is detailed as follows.

1) Data Preprocess and RF-Based Model Structure Construction: After collecting interested battery manufacturing data, the obvious outliers of original data are first removed and the suitable class labels of outputs are set. In this article, both the battery electrode mass load and porosity are classified with five class

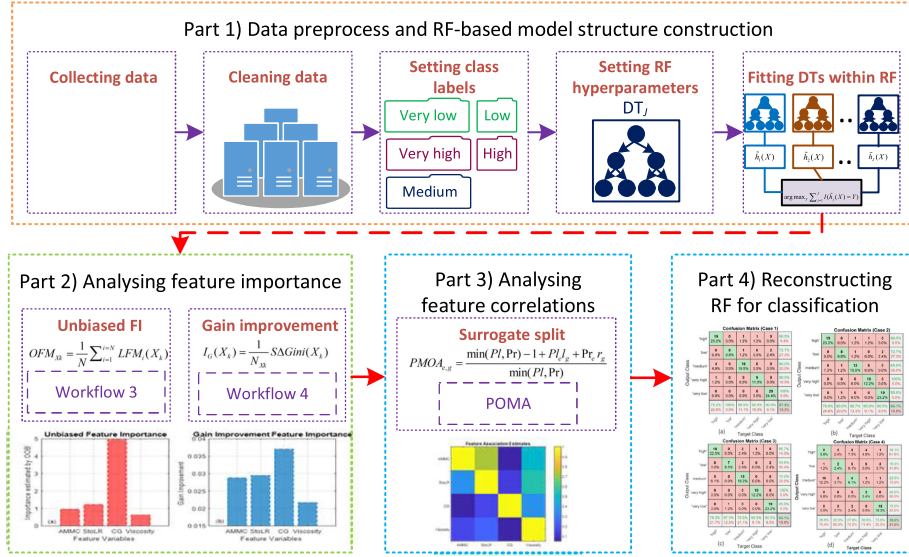


Fig. 5. Total framework to design RF-based model for classifying and analyzing features importance, as well as correlations.

labels. Then, the preprocessed input–output observations are utilized to train all DTs within RF through the steps in Workflow 1. As the RF model is a powerful but easy-to-use machine learning method with only two hyperparameters [the number of DTs (J) and the amount of features in each split (m)] to tune, some key points should be considered in this stage. First, for J , in theory, with higher number of DTs, a larger accuracy and generalization ability is obtained. However, too many DTs would highly increase the computational effort of RF. Second, m would affect the performance of each DT and the correlations among any DTs within RF. Large m benefits the strength of each DT but also makes all DTs become more correlated. In our study, these hyperparameters are tuned by an effective method named randomized search [34].

2) *Analyzing Feature Importance*: In this part, to quantify all interested FI and analyze their effects on the classification performance of electrode mass load and porosity, two effective quantitative indicators, including the unbiased FI and the gain improvement FI, are utilized. Specifically, the unbiased FI is calculated by permuting OOB observations with the detailed process in Workflow 3, while the gain improvement FI is obtained by summing Gini changes caused by splits on each feature (Workflow 4).

3) *Analyzing Feature Correlations*: After quantifying the importance of mixing and coating features, the PMOAs values of each feature pair are calculated by (1) and plotted as an $M \times M$ heat map. Then, the correlations between each two features can be analyzed by these PMOAs. In theory, larger PMOAs indicate that there exist more highly correlations between feature pairs. In the heat map, the PMOAs of two features would be different, depending on which feature first generates the optimal split within DTs.

4) *Reconstructing RF for Classification*: After comparing the FI and analyzing feature correlations, the most important features that affect classification results are selected. Then, the

RF can be reconstructed with a reduced feature set for new classifications.

Following this framework, an effective RF-model-based framework can be formulated to not only analyze the importance and correlations of mixing and coating features, but also well classify the manufactured battery electrode mass load and porosity into suitable categories. Besides, after collecting more PPs, IPFs, and product properties of a battery manufacturing chain, this framework can be further extended to analyze data correlations, discover most important features, and simplify model structure with a reduced variable set.

D. Performance Metrics

In this subsection, to compare and quantify the classification performance of the designed RFs, several performance metrics, including the CM, macro-precision, macro-recall, as well as macro F1-score, are applied in this study.

In classification applications, let positive correspond to the interested class while negative correspond to other classes; four basic measures, including true positives (TP), false positives (FP), true negatives (TN), and false negatives (FN), can be formulated for each class. For an interested class c_h (here $h = 1 : 5$), the precision rate (P_{rate}) can be used to quantify the correct classification results of this class as

$$P_{rate}(c_h) = \frac{TP}{TP + FP}. \quad (2)$$

Recall rate (R_{rate}) could quantify the rate of all fraud conditions of this class as

$$R_{rate}(c_h) = \frac{TP}{TP + FN}. \quad (3)$$

F-measure ($F_{measure}$) reflects the harmonic mean of precision and recall of this class as

$$F_{measure}(c_h) = \frac{2 \times P_{rate}(c_h) \times R_{rate}(c_h)}{P_{rate}(c_h) + R_{rate}(c_h)}. \quad (4)$$

The overall correct classification rate (*OCCrate*) to reflect the proportion of correctly classified observations out of all the observations is calculated by

$$OCCrate = \frac{TP_{all} + TN_{all}}{N} \quad (5)$$

where $TP_{all} + TN_{all}$ represent all outputs that have been correctly classified, and N is the total number of observations.

Based upon the aforementioned metrics, an $(M+1) \times (M+1)$ CM of multiclass issue could be formulated. Each row within CM reflects the predicted output class, while each column stands for the actual target class. The elements on the primary diagonal are the correct results, while other elements reflect the incorrect classification cases. The $(M+1)$ th column and row represent the $Prate(c_h)$ and $Rrate(c_h)$ of each class, respectively. The last element in the bottom right corner represents the *OCCrate*.

Supposing that each class has a $Prate(c_h)$, $Rrate(c_h)$, and $Fmeasure(c_h)$, then the macro-precision (*macroP*), macro-recall (*macroR*), and macro F1-score (*macroF1*) can be calculated to evaluate the overall classification performance of our battery manufacturing multiclass issue as

$$\begin{cases} \text{macroP} = \sum_{h=1}^5 Prate(c_h)/5 \\ \text{macroR} = \sum_{h=1}^5 Rrate(c_h)/5 \\ \text{macroF1} = \sum_{h=1}^5 Fmeasure(c_h)/5 \end{cases}. \quad (6)$$

IV. RESULTS AND DISCUSSIONS

To well quantify FI, feature correlations, and their effects on the classification of electrode properties, the designed RF-based framework is utilized to classify both battery electrode mass load and porosity in this section.

A. RF Classification Model for Battery Mass Load

In this test, based upon the structure, as illustrated in Fig 4, four features, including AMMC, StoLR, viscosity, and CG, are utilized as the inputs of the RF model, while the labeled electrode mass load is used as model's output. Then, the detailed results of FI, correlations, RF-based model classification, and performance comparison would be given and analyzed.

1) Feature Analyses: For the mass load classification, following the steps in Workflows 3 and 4, the quantified unbiased FI as well as gain improvement FI of all four feature variables can be obtained and illustrated in Fig. 6. It can be noted that although the value levels between unbiased FI and gain improvement FI are significantly different, they still present the similar trend for all features. Obviously, CG achieves much higher importance values for both unbiased FI (here is 4.78) and gain improvement FI (here is 0.037), indicating that this variable is the most important feature for mass load classification. StoLR and AMMC provide the second and third larger values of both unbiased FI (here are 1.18 and 0.91, respectively) as well as gain improvement FI (here are 0.029 and 0.028, respectively). The viscosity variable presents the smallest values with 0.67 unbiased FI and 0.022 gain improvement FI, indicating that this feature contributes the least to the classification of electrode mass load.

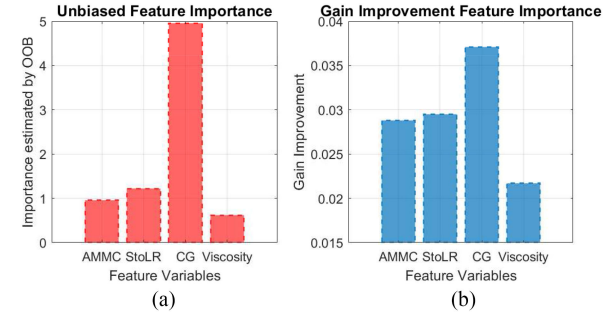


Fig. 6. FI for battery mass load. (a) Unbiased FI based on OOB. (b) FI based on gain improvement.

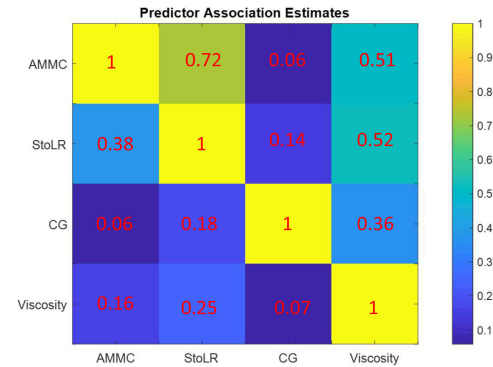


Fig. 7. Heat map to reflect feature correlations for battery mass load case.

The PMOAs of all feature pairs are calculated next to evaluate the correlations among four features for mass load case. From the heat map in Fig. 7, the largest correlation occurs between AMMC and StoLR with a PMOA of 0.72. This correlation output is very useful as the obtained result is consistent with the conclusion from experimental works [35], but we demonstrate how an RF machine learning framework can aid the interpretation of correlations among feature variables of interest, which could give engineers a guidance to efficiently understand their battery manufacturing chain.

2) RF-Based Model: To evaluate the mass load classification results of our proposed RF framework, the prediction test through using all features is first carried out. According to the corresponding CM in Fig. 8, a satisfactory *OCCrate* with 90.2% is achieved. Quantitatively, the classes “very high” and “very low” achieve 100% *Prate*. The worst classification result is the “low” class with 72.7% *Prate*. This is mainly caused by two observations, which are incorrectly classified as “very low” and “medium.”

3) Performance Comparison: Next, to further investigate the effects of each feature on the mass load classification results, four different cases with various combinations of three features are tested and compared. Specifically, Case 1 consists of CG, AMMC, and StoLR features. Case 2 contains CG, AMMC, and viscosity features. Case 3 includes CG, StoLR, and viscosity features. Case 4 is composed of AMMC, StoLR, and viscosity features. Fig. 9 and Table II illustrate the corresponding CMs

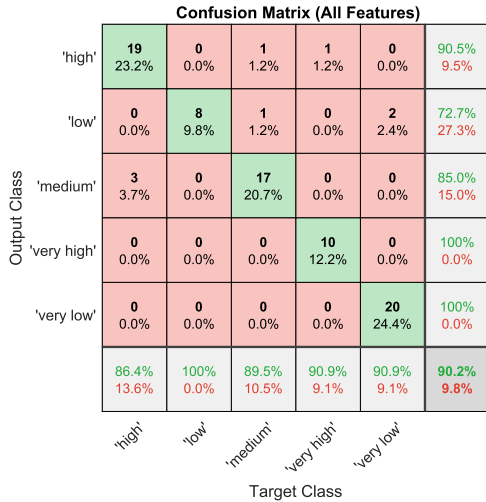


Fig. 8. CM for mass load results by using all features.

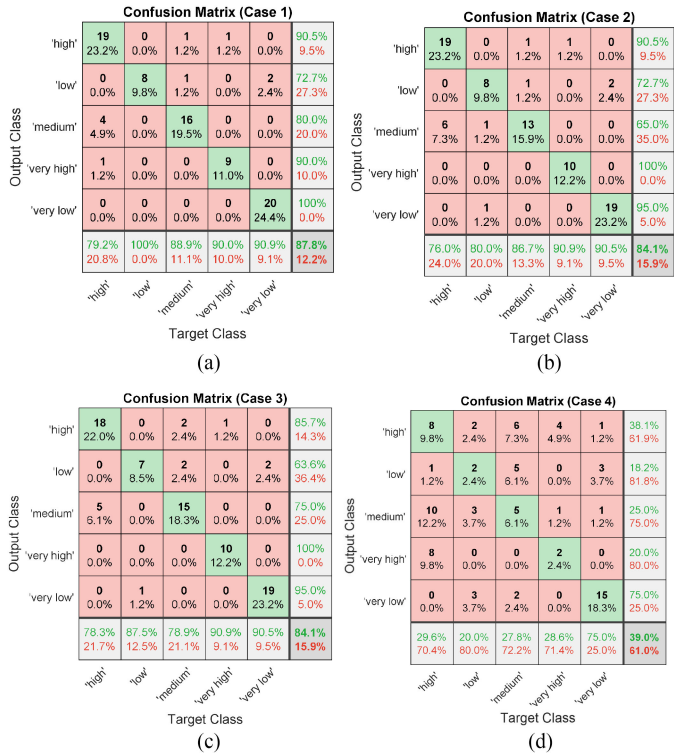


Fig. 9. Confusion matrices for mass load classification results for different cases: (a) Case 1, (b) Case 2, (c) Case 3, and (d) Case 4.

TABLE II
QUANTITATIVE PERFORMANCE METRICS FOR BATTERY ELECTRODE MASS LOAD CLASSIFICATION

Cases.	<i>macroP</i>	<i>macroR</i>	<i>macroF1</i>
All features	89.6%	91.5%	90.1%
Case 1	86.6%	89.8%	90.0%
Case 2	84.6%	84.8%	84.6%
Case 3	83.9%	85.2%	84.3%
Case 4	35.3%	36.2%	35.4%

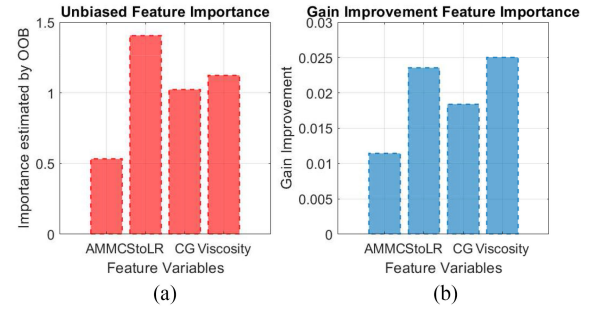


Fig. 10. FI for battery porosity. (a) Unbiased FI based on OOB. (b) FI based on gain improvement.

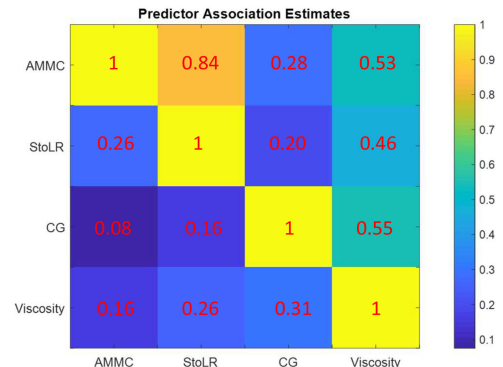


Fig. 11. Heat map to reflect feature correlations for battery porosity case.

and performance metrics of all cases. It can be seen that Case 1 provides the best classification results with 86.6% *macroP*, 89.8% *macroR*, and 90.0% *macroF1*, which are only 3.3%, 1.9%, and 0.1% less than those from the case of all features. This implies that using CG, AMMC, and StoLR is sufficient for mass load classification. Cases 2 and 3 provide the similar performance metrics, which indicates that similar effects exist between AMMC and StoLR. Interestingly, without involving CG, the performance metrics of Case 4 largely decrease, indicating that CG plays a significantly important role in the mass load classification.

B. RF Classification Model for Battery Porosity

Next, the battery electrode porosity classification test is also conducted. The inputs of this test are the same as those from mass load test, while the output here becomes porosity.

1) Feature Analyses: Fig. 10 illustrates the corresponding unbiased FI and gain improvement FI. The metrics indicate that StoLR and viscosity are the two most contributing features, while AMMC is the worst one. Next, from the association estimates of corresponding feature pairs in Fig. 11, one PMOA of the AMMC-StoLR pair presents the highest value with 0.84, indicating that these two features have strong potential correlations for the battery electrode porosity classification case.

2) RF-Based Model: Fig. 12 illustrates the CM for the porosity classification results when using all features. This test

Confusion Matrix (All Features)							
Output Class	'high'	2 2.4%	1 1.2%	3 3.7%	1 1.2%	0 0.0%	28.6% 71.4%
	'low'	0 0.0%	30 36.6%	3 3.7%	0 0.0%	4 4.9%	81.1% 18.9%
	'medium'	2 2.4%	4 4.9%	9 11.0%	0 0.0%	0 0.0%	60.0% 40.0%
	'very high'	1 1.2%	1 1.2%	0 0.0%	3 3.7%	0 0.0%	60.0% 40.0%
	'very low'	0 0.0%	4 4.9%	0 0.0%	14 17.1%	77.8% 22.2%	70.7% 29.3%
	40.0% 60.0%	75.0% 25.0%	60.0% 40.0%	75.0% 25.0%	77.8% 22.2%	70.7% 29.3%	
Target Class							

Fig. 12. CM for porosity results by using all features.

TABLE III
QUANTITATIVE PERFORMANCE METRICS FOR BATTERY ELECTRODE POROSITY CLASSIFICATION

Cases.	macroP	macroR	macroF1
All features	61.5%	65.6%	66.4%
Case 1	54.9%	54.7%	54.9%
Case 2	53.8%	48.3%	50.6%
Case 3	59.4%	60.8%	59.7%
Case 4	67.2%	56.8%	54.6%

achieves a classification result with 70.7% *OCCRate*, which is mainly caused by several misclassified results such as those with class label “high.” In comparison with the battery mass load case, it can be concluded that these features cannot fully and well determine the qualities of electrode porosity.

3) Performance Comparison: To further investigate the influence of these features on the electrode porosity classifications, four tests with the same feature combination cases as those from mass load are compared here. Their corresponding CMs and performance metrics are shown in Fig. 13 and Table III, respectively. Specifically, by using the three most important features (StoLR, CG, and viscosity), Case 3 achieves the best classification results with 59.4% *macroP*, 60.8% *macroR*, 59.7% *macroF1*, and 68.3% *OCCRate*. In contrast, using AMMC to replace any other three features, the related classification performance is reduced accordingly. However, the overall porosity classification results are all worse than those from mass load cases. These facts signify that for battery electrode porosity, more other related IPFs and PPs are recommended to be considered for further improving its classification performance.

C. Discussions

In this subsection, two tests are designed to investigate the hyperparameter tuning and compare the performance of the proposed RF with other typical classification methods, followed by the further discussions of results in Sections IV-A and IV-B.

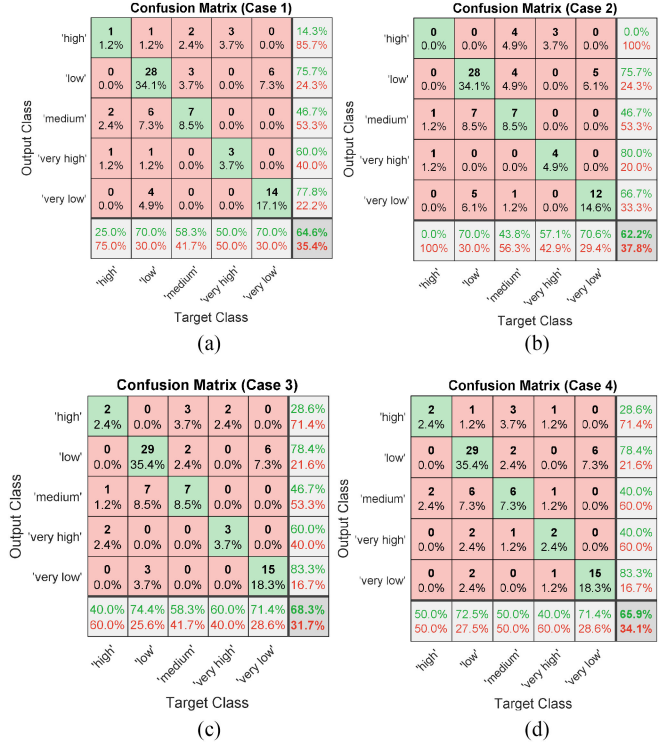


Fig. 13. Confusion matrices for porosity classification results for different cases: (a) Case 1, (b) Case 2, (c) Case 3, and (d) Case 4.

TABLE IV
RESULTS OF HYPERPARAMETER TUNING

Hyper-parameter combinations	MCVA (mass load)	MCVA (porosity)
$J = 40, m = 2$	88.0%	62.2%
$J = 60, m = 2$	88.5%	64.8%
$J = 80, m = 2$	88.8%	66.1%
$J = 100, m = 2$	89.8%	68.1%
$J = 120, m = 2$	90.0%	69.3%
$J = 40, m = 3$	88.6%	62.5%
$J = 60, m = 3$	69.1%	65.3%
$J = 80, m = 3$	90.0%	70.6%
$J = 100, m = 3$	90.2%	70.5%
$J = 120, m = 3$	90.2%	70.6%

1) Hyperparameter Tuning: As mentioned in Section III-C, for the RF classification model, J and m are two key hyperparameters required to be carefully tuned. Through setting up random combinations to train model and score the mean cross-validated accuracy (MCVA), the randomized search solution [34] is utilized here to determine suitable values of J and m for both electrode mass load and porosity classification cases. Based upon the Python module Scikit-learn with a 2.40-GHz Intel Pentium 4 CPU, the randomized search can be conveniently carried out by using the function module *RandomizedSearchCV*. In our study, the search range of J is set as *range*(40, 120, 20), while the candidates of m is [2,3], respectively. Table IV illustrates the classification performance with various hyperparameter combinations. It can be seen that $J = 100, m = 3$ presents the best MCVA with 90.2% for the mass load case, while $J = 80, m = 3$ provides the best MCVA

TABLE V
CLASSIFICATION RESULTS USING VARIOUS APPROACHES

Approaches	Mass load		Porosity	
	<i>macroF1</i>	AUC	<i>macroF1</i>	AUC
DT	74.6%	0.82	53.2%	0.77
KNN	83.9%	0.92	56.4%	0.81
SVM	89.8%	0.98	66.0%	0.93
proposed RF	90.1%	0.98	66.4%	0.94

with 70.6% for the porosity case. Therefore, the related RF classification models are set with these optimized hyperparameters in our study.

2) Comparisons With Other Approaches: To further reflect the effectiveness of our designed RF model, another three popular classification approaches, including the DT, k-nearest neighbors (KNN), and SVM, are utilized as the benchmarks for comparison purpose. Specifically, DT is a solo CART. KNN belongs to an instance-based learning method and relies on the distance for classification. SVM is a kernel-based method to map inputs into high-dimensional spaces for classification [36]. Without loss of generality, randomized search solution is also utilized here to tune their hyperparameters. After optimization, DT has the maximum split number of 20. The neighbor number of KNN is 1; SVM uses the Gaussian kernel with a kernel scale of 0.5. To quantify their classification performance, two significant metrics, including the *macroF1* and the area under curve (AUC) of receiver operating characteristic, are utilized. Here, the AUC could give the degree or measure of separability of the classes [37]. Table V illustrates the classification results of all these approaches after fivefold cross-validation. It can be seen that DT shows the worst results, while SVM and RF provide good classification results for both mass load and porosity cases (here, RF provides a slightly better *macroF1* and AUC). Therefore, due to the ensemble learning nature, our proposed RF framework presents competent performance in the classification applications of battery manufacturing.

3) Further Discussions: Due to the lack of exploiting interpretable data-driven solutions for feature analyses and modeling within the battery manufacturing chain, this article develops an RF-based framework to quantify variable correlations and importance in the classification of battery electrode properties. According to the obtained results from Sections IV-A and IV-B, the electrode mass load can be well determined by the investigated four features (here the *macroF1* is 90.1%), while CG plays the most important role in its classification results (nearly 60.7% decrease). This result is expected as CG would significantly affect the coating weight and thickness, and these coating properties highly determine the electrode mass load. For the results of electrode porosity, the *macroF1* here is just 66.4%, indicating that more other feature variables should be considered to better classify the electrode porosity. This result is expected as electrode porosity would also be highly affected by the drying parameters (rate, temperature, pressure, etc.) in theory. Not surprisingly, AMMC and StoLR present high correlation for both mass load and porosity cases. This is mainly due to the mass ratio between slurry solid components, and slurry mass has

strong and direct relations with the active material properties. In contrast, there are not so direct relations for other feature pairs, which leads to that their correlations become less. Besides, the mass content of active material cannot highly affect the electrode physical property such as porosity, which makes the AMMC here become the less important feature. In light of this, to further improve our proposed RF-based framework for better prediction of electrode porosity, more feature variables from drying and calendering processes such as drying rate, temperature, pressure, and calendering speed should be considered. Besides, more available data from other key production processes could also be collected to improve the interpretability of the RF model for better understanding battery manufacturing.

V. CONCLUSION

As battery manufacturing is crucial for determining battery performance, the effective feature analyses and electrode property classification within manufacturing chain are strongly required. In this article, through using the improved RF technique, a powerful data-driven framework is designed to not only quantify the importance levels of four key battery manufacturing features but also provide their feature association estimates. The effects of AMMC, StoLR, CG, and viscosity on the classifications of both electrode mass load and porosity are all evaluated and analyzed. Due to the superiority in terms of interpretability and data-driven nature, the proposed RF classification framework could be conveniently extended to consider more input features from other key manufacturing stages such as mixing, drying, and calendering. As collecting battery manufacturing data requires specific equipment and is time-consuming, our future work would focus on designing extra experiments to generate more related data such as the mixing kneading intensity and speed, the drying rate, temperature and pressure, and the calendering speed and then to further improve the usability of such a machine learning method and accelerate the development of high-performance Li-ion batteries.

REFERENCES

- [1] D. L. Wood, III, J. Li, and S. J. An, "Formation challenges of lithium-ion battery manufacturing," *Joule*, vol. 3, no. 12, pp. 2884–2888, 2019.
- [2] O. Schmidt, M. Thomitzek, F. Röder, S. Thiede, C. Herrmann, and U. Kreuer, "Modeling the impact of manufacturing uncertainties on lithium-ion batteries," *J. Electrochem. Soc.*, vol. 167, no. 6, 2020, Art. no. 060501.
- [3] M. Ghahramani, Y. Qiao, M. Zhou, A. O. Hagan, and J. Sweeney, "Ai-based modeling and data-driven evaluation for smart manufacturing processes," *IEEE/CAA J. Autom. Sinica*, vol. 7, no. 4, pp. 1026–1037, Jul. 2020.
- [4] M. A. Saez, F. P. Maturana, K. Barton, and D. M. Tilbury, "Context-sensitive modeling and analysis of cyber-physical manufacturing systems for anomaly detection and diagnosis," *IEEE Trans. Autom. Sci. Eng.*, vol. 17, no. 1, pp. 29–40, Jan. 2020.
- [5] C. Zhang, Y. Zhang, and Y. Li, "A novel battery state-of-health estimation method for hybrid electric vehicles," *IEEE/ASME Trans. Mechatronics*, vol. 20, no. 5, pp. 2604–2612, Oct. 2015.
- [6] X. Hu, F. Feng, K. Liu, L. Zhang, J. Xie, and B. Liu, "State estimation for advanced battery management: Key challenges and future trends," *Renewable Sustain. Energy Rev.*, vol. 114, 2019, Art. no. 109334.
- [7] F. Feng *et al.*, "Co-estimation of lithium-ion battery state of charge and state of temperature based on a hybrid electrochemical-thermal-neural-network model," *J. Power Sources*, vol. 455, 2020, Art. no. 227935.

- [8] Y. Wang *et al.*, “A comprehensive review of battery modeling and state estimation approaches for advanced battery management systems,” *Renewable Sustain. Energy Rev.*, vol. 131, 2020, Art. no. 110015.
- [9] Y. Li *et al.*, “Data-driven health estimation and lifetime prediction of lithium-ion batteries: A review,” *Renewable Sustain. Energy Rev.*, vol. 113, 2019, Art. no. 109254.
- [10] X. Hu, Y. Che, X. Lin, and Z. Deng, “Health prognosis for electric vehicle battery packs: A data-driven approach,” *IEEE/ASME Trans. Mechatronics*, vol. 25, no. 6, pp. 2622–2632, Dec. 2020.
- [11] K. Liu, X. Hu, Z. Wei, Y. Li, and Y. Jiang, “Modified Gaussian process regression models for cyclic capacity prediction of lithium-ion batteries,” *IEEE Trans. Transp. Electricit.*, vol. 5, no. 4, pp. 1225–1236, Dec. 2019.
- [12] K. Liu, Y. Li, X. Hu, M. Lucu, and D. Widanalage, “Gaussian process regression with automatic relevance determination kernel for calendar aging prediction of lithium-ion batteries,” *IEEE Trans. Ind. Inform.*, vol. 16, no. 6, pp. 3767–3777, Jun. 2020.
- [13] X. Hu, K. Zhang, K. Liu, X. Lin, S. Dey, and S. Onori, “Advanced fault diagnosis for lithium-ion battery systems: A review of fault mechanisms, fault features, and diagnosis procedures,” *IEEE Ind. Electron. Mag.*, vol. 14, no. 3, pp. 65–91, Sep. 2020.
- [14] Q. Ouyang, Z. Wang, K. Liu, G. Xu, and Y. Li, “Optimal charging control for lithium-ion battery packs: A distributed average tracking approach,” *IEEE Trans. Ind. Inform.*, vol. 16, no. 5, pp. 3430–3438, May 2020.
- [15] C. Zou, C. Manzie, and D. Nešić, “Model predictive control for lithium-ion battery optimal charging,” *IEEE/ASME Trans. Mechatronics*, vol. 23, no. 2, pp. 947–957, Apr. 2018.
- [16] K. Liu, C. Zou, K. Li, and T. Wik, “Charging pattern optimization for lithium-ion batteries with an electrothermal-aging model,” *IEEE Trans. Ind. Inform.*, vol. 14, no. 12, pp. 5463–5474, Dec. 2018.
- [17] Y. Shang, K. Liu, N. Cui, N. Wang, K. Li, and C. Zhang, “A compact resonant switched-capacitor heater for lithium-ion battery self-heating at low temperatures,” *IEEE Trans. Power Electron.*, vol. 35, no. 7, pp. 7134–7144, Jul. 2020.
- [18] X. Dai, Q. Quan, J. Ren, and K.-Y. Cai, “An analytical design-optimization method for electric propulsion systems of multicopter UAVs with desired hovering endurance,” *IEEE/ASME Trans. Mechatronics*, vol. 24, no. 1, pp. 228–239, Feb. 2019.
- [19] T. Knoche, F. Surek, and G. Reinhart, “A process model for the electrolyte filling of lithium-ion batteries,” *Procedia CIRP*, vol. 41, pp. 405–410, 2016.
- [20] J.-H. Schünemann, H. Dreger, H. Bockholt, and A. Kwade, “Smart electrode processing for battery cost reduction,” *ECS Trans.*, vol. 73, no. 1, pp. 153–159, 2016.
- [21] T. Günther, D. Schreiner, A. Metkar, C. Meyer, A. Kwade, and G. Reinhart, “Classification of calendering-induced electrode defects and their influence on subsequent processes of lithium-ion battery production,” *Energy Technol.*, vol. 8, 2019, Art. no. 1900026.
- [22] J. Schnell and G. Reinhart, “Quality management for battery production: A quality gate concept,” *Procedia CIRP*, vol. 57, pp. 568–573, 2016.
- [23] J. Schnell *et al.*, “Data mining in lithium-ion battery cell production,” *J. Power Sources*, vol. 413, pp. 360–366, 2019.
- [24] A. Turetskyy, S. Thiede, M. Thomitzek, N. von Drachenfels, T. Pape, and C. Herrmann, “Toward data-driven applications in lithium-ion battery cell manufacturing,” *Energy Technol.*, 2019, Art. no. 1900136.
- [25] S. Thiede, A. Turetskyy, A. Kwade, S. Kara, and C. Herrmann, “Data mining in battery production chains towards multi-criterial quality prediction,” *CIRP Ann.*, vol. 68, no. 1, pp. 463–466, 2019.
- [26] T. Kornas *et al.*, “A multivariate KPI-based method for quality assurance in lithium-ion-battery production,” *Procedia CIRP*, vol. 81, pp. 75–80, 2019.
- [27] L. Hoffmann *et al.*, “Capacity distribution of large lithium-ion battery pouch cells in context with pilot production processes,” *Energy Technol.*, vol. 8, 2019, Art. no. 1900196.
- [28] R. P. Cunha, T. Lombardo, E. N. Primo, and A. A. Franco, “Artificial intelligence investigation of NMC cathode manufacturing parameters interdependencies,” *Batteries Supercaps*, vol. 3, no. 1, pp. 60–67, 2020.
- [29] A. Kwade, W. Haselrieder, R. Leithoff, A. Modlinger, F. Dietrich, and K. Droeder, “Current status and challenges for automotive battery production technologies,” *Nat. Energy*, vol. 3, no. 4, pp. 290–300, 2018.
- [30] A. Cutler, D. R. Cutler, and J. R. Stevens, “Random forests,” in *Ensemble Machine Learning*. Berlin, Germany: Springer, 2012, pp. 157–175.
- [31] A. Liaw and M. Wiener, “Classification and regression by randomForest,” *R News*, vol. 2, no. 3, pp. 18–22, 2002.
- [32] Y. Li *et al.*, “Random forest regression for online capacity estimation of lithium-ion batteries,” *Appl. Energy*, vol. 232, pp. 197–210, 2018.
- [33] S. Nembrini, I. R. König, and M. N. Wright, “The revival of the Gini importance?,” *Bioinformatics*, vol. 34, no. 21, pp. 3711–3718, 2018.
- [34] J. Bergstra and Y. Bengio, “Random search for hyper-parameter optimization,” *J. Mach. Learn. Res.*, vol. 13, no. 1, pp. 281–305, 2012.
- [35] E. Kendrick, “Advancements in manufacturing,” in *Future Lithium-Ion Batteries*. London, U.K.: Royal Society of Chemistry, 2019, pp. 262–289.
- [36] Y. Zhang *et al.*, “Comparison of machine learning methods for stationary wavelet entropy-based multiple sclerosis detection: Decision tree, k-nearest neighbors, and support vector machine,” *Simulation*, vol. 92, no. 9, pp. 861–871, 2016.
- [37] G. Biau and E. Scornet, “A random forest guided tour,” *Test*, vol. 25, no. 2, pp. 197–227, 2016.



Kailong Liu (Member, IEEE) received the Ph.D. degree in electrical engineering from Queen's University Belfast (QUB), Belfast, U.K., in 2018.

He is currently a Senior Research Fellow with the Warwick Manufacturing Group, University of Warwick, Coventry, U.K. He was a Visiting Student Researcher with Tsinghua University, Beijing, China, in 2016. His research interests include modeling, optimization, and control with applications to electrical/hybrid vehicles, energy storage, battery manufacture, and

management.

Dr. Liu was the Student Chair of the IEEE QUB student branch and a recipient of awards such as EPSRC, Santander, and QUB ESM International Scholarships.



Xiaosong Hu (Senior Member, IEEE) received the Ph.D. degree in automotive engineering from the Beijing Institute of Technology, Beijing, China, in 2012.

He is currently a Professor with the State Key Laboratory of Mechanical Transmissions and the Department of Automotive Engineering, Chongqing University, Chongqing, China. He has authored or coauthored more than 100 high-caliber journal/conference papers. His research interests include battery technologies and modeling and controls of electrified vehicles.

Dr. Hu is a recipient of several prestigious awards/honors, including the SAE Ralph Teeter Educational Award in 2019, the Emerging Sustainability Leaders Award in 2016, and the EU Marie Curie Fellowship.



Huiyu Zhou received the B.Eng. degree in radio technology from the Huazhong University of Science and Technology, Hefei, China, the M.Sc. degree in biomedical engineering from the University of Dundee, Dundee, U.K., and the Dr.Phil. degree in computer vision from Heriot-Watt University, Edinburgh, U.K.

He is currently a Professor with the Department of Informatics, University of Leicester, Leicester, U.K. He has authored or coauthored more than 270 peer-reviewed papers. His research work has been or is being supported by the U.K. Engineering and Physical Sciences Research Council, the Medical Research Council, European Union, Royal Society, Leverhulme Trust, Puffin Trust, Invest NI, and industry.



Lei Tong received the M.Phil. degree in computer science in 2020 from the University of Leicester, Leicester, U.K., where he is currently working toward the Ph.D. degree with the Department of Informatics.

His current research interests include natural language processing, computer vision, and data mining.



James Marco received the Eng.D. degree from the University of Warwick, Coventry, U.K., in 2000.

He worked for several years within the automotive industry leading engineering research teams for Ford (North America and Europe), Jaguar Cars, Land Rover, and DaimlerChrysler (Germany). He is currently a Professor of Systems Modeling and Control with the University of Warwick. His research interests include systems engineering, real-time control, energy storage

modeling, and design optimization.

Mr. Marco is a Chartered Engineer and a Fellow of the Institution of Engineering and Technology.



W. Dhammika Widanage (Member, IEEE) is an Associate Professor of Modeling and Energy Storage with the Warwick Manufacturing Group (WMG), University of Warwick, Coventry, U.K. His research interests include system identification theory, applied across several applications including batteries. He leads battery modeling research in the department and recently secured funding to lead the modeling activity as a Principal Investigator (PI) (for WMG) on the Faraday Multiscale Modelling project, as a Co-Investigator (Co-I) on the EPSRC Prosperity Partnership with Jaguar Land Rover and a PI and Co-I on four Innovate U.K. projects (PI and three Co-I).

Dr. Widanage was the recipient of the WMG Early Career Researcher of the Year Award in 2016.